

Fragmentation: The Zonation Method Applied to Fragmented Human Remains from Archaeological and Forensic Contexts

Christopher J. Knüsel and Alan K. Outram

Abstract

Scattered and commingled human and animal remains are commonly encountered on archaeological sites, and this contextual relationship begs the question of whether human and animals were treated in a similar manner before burial. The recording system presented here provides a means by which to confront problems of equifinality – that is, when taphonomic alterations create apparently similar patterns and, therefore, confuse behavioural inferences drawn from them. This method hinges on a standardised representation of the zones on human skeletal elements that allow comparison with those described by Dobney and Rielly (1988) for animal remains. It is anticipated that the anatomical descriptions in combination with the zone drawings presented will aid others to apply the method generally across skeletal assemblages of any date. This system could also be used to aid the curation of museum collections and as a complement to forensic recovery.

Keywords: ZONATION METHOD, HUMAN REMAINS, FRAGMENTATION

Introduction

Recording systems for human remains are based on the recovery of a more or less complete individual in an isolated context (see, for example, Buikstra and Ubelaker 1994). These systems do not easily lend themselves to the fragmentary human remains that are often encountered on archaeological sites, let alone in many forensic contexts, where post-mortem events, including dismemberment and subsequent animal scavenging, result in scattered, disarticulated and fragmentary human remains. The same can be said of medieval charnel deposits that resulted from the occasional disturbance and tidying up of crowded medieval parish churchyard burials, where the commingled remains of numerous individuals, occasionally sorted by major skeletal element, as in some church crypts, create a similar pattern. These methods are especially difficult to

apply to the grand majority of funerary contexts encountered in sites of later European prehistoric date, which do not involve the inhumation of complete human bodies in a primary, undisturbed context (see, for example, Carr and Knüsel 1997). Scattered human remains on these sites have often been interpreted as relating to a variety of funerary rites, including above-ground exposure and excarnation, secondary burial, excarnation by defleshing, or trophy collecting and dismemberment, as well as disturbance of primary burials through the post-mortem intervention of humans or taphonomic processes relating to animal, geological, or biological actions. The recording system presented here provides a means by which to confront problems of equifinality – that is, when taphonomic alterations create apparently similar patterns and, therefore,

Received August 2003, revised manuscript accepted September 2003.

Authors' Addresses: Christopher J. Knüsel, Biological Anthropology Research Centre (BARC), Department of Archaeological Sciences, University of Bradford, Bradford, West Yorkshire, BD7 1DP, UK, Email: c.knusel@bradford.ac.uk; Alan K. Outram, Department of Archaeology, School of Geography, Archaeology, and Earth Resources, University of Exeter, Laver Building, North Park Road, Exeter, EX4 4QE, UK, Email: a.k.outram@exeter.ac.uk

confuse behavioural inferences drawn from them.

In addition, due to inadequate excavation and/or curation strategies, other human material has upon occasion also become commingled, sometimes scattered among repositories and fragmented. If such material is inadequately recorded or unlabelled, there is no completely reliable way to recover individuals from such material. In these instances, researchers adopt techniques more often applied in faunal studies in order to gauge population size and frequencies of those individuals of a certain sex, age, anatomical trait, or pathological condition. When commingled skeletons are encountered, researchers often employ a MNI (Minimum Number of Individuals) count based on the number of recognisable non-repeatable articulations (i.e., those that can occur no more than once in a given element) to ascertain a conservative estimate of the numbers of individuals contributing to a given assemblage (Klein and Cruz-Urbe 1984). The alternative is to provide a NISP (Number of Identifiable Specimens) count, a procedure that assumes that each recognisable fragment may represent an individual and thus produces a potentially inflated estimate of the numbers contributing to an assemblage (Klein and Cruz-Urbe 1984). The combination of these two procedures provides a minimum and maximum number of individuals represented in a given assemblage.

The following paper presents a recording system developed to deal with scattered, fragmented human remains. Based on the zonation method of Dobney and Rielly (1988), and when combined with Minimum Number of Elements (MNE) counts (as defined by Binford 1984), this system provides the means to employ indices of fragmentation such as Morlan's (1994) 'Percent Completeness'. This percentage is determined by working out the average number of zones per bone element, and making this number into a percentage count using the maximum possible number of zones per element. This method provides a means by which to quantify the breakage of bone by element, which can be used in conjunction with analysis of fracture types when investigating the extent, nature and sequence of breakage. The application of such a method presents a more accurate record of the human remains recovered in commingled, disarticulated and fragmented assemblages.

Dobney and Rielly's (1988) zonation method is an apt system to adopt because it allows the accurate recording of a single bone fragment such that it can be compared with other fragments from similar elements, as well as those from a variety of species that commonly occur on archaeological sites. Dobney and Rielly's (1988) zones are based on the commonly occurring fragments recovered in ar-

chaeological faunal assemblages and, importantly, the system provides for recording of whole bones, including the diaphyses that are often ignored or more vaguely accounted for in other recording systems. Dobney and Rielly (1988, 81) created their method 'to include all the economically important domestic animals', and thus did not include humans. The value of a recording method for use with both human and non-human material is that the frequencies of individual zones can be compared directly between domestic animals and humans, a comparison upon which many arguments about past behaviour hinges, such as those documenting cannibalism, sacrifice, or others where humans and animals may be suspected of being treated in a similar fashion.

Methods

Dobney and Rielly's (1988) zone drawings and written descriptions of the zones were used to inform the zones developed for human remains. Where there was an inconsistency between the written description and the drawing, we opted to use the drawing as the template for the present system (the descriptions for the femoral condyles are reversed in Dobney and Rielly's (1988) original fig. 12). Following Dobney and Rielly (1988), we employed standard anatomical names for identifiable regions of human bones and adjusted the descriptions to account for the placement of tendinous and ligamentous attachments and other surface anatomical features of human skeletal elements. The application of this procedure means that some of the original terms in Dobney and Rielly's (1988) descriptions have been altered (e.g. the placement of the *tuberculum teres* of zone 10 of the humerus in the quadruped, Dobney and Rielly's (1988) original fig. 9, is not equivalent to the attachment of *M. teres major* in the human humerus). Again, in these cases, we favoured the position of the zone in the drawings, sometimes basing these on comparative proportions of the human and non-human morphology. In each case, we always maintained the same number of zones, although this meant that in the case of the proximal ulna, we recorded two zones for fragments possessing the proximal end – zones A and B of the human olecranon process – due to the presence of a projecting olecranon process in animals (Dobney and Rielly 1988, fig. 10) that is not found in humans.

For bones that are retained in a plesiomorphic condition in humans and therefore not accounted for in Dobney and Rielly's (1988) method, for example, the retention of a clavicle and an unfused fibula in the human skeleton, we devised zones to

cover these elements, as well as those covering the sternum. The metapodials and phalanges were recorded as either pedal or manual. We followed Dobney and Rielly's (1988) zones for the pig metapodials for humans, avoiding the recording method for artiodactyl metapodials (with their reduced number) in the process. Dobney and Rielly (1988) suggested that the cranium could be divided into zones, but did not do so in their study. We did so, in order to record not only fragmentation but also to identify the position of cranial lesions and injuries.¹

Tarsals and carpals, as well as patellae, are recorded as one zone and as left or right, although these could be divided if the research protocol demanded. The hyoid and throat cartilages (cricoid and thyroid cartilages) are recorded as such, although these could be divided if the research protocol demanded it (for example, the hyoid could be divided into right and left cornua and the body). The recording of sub-adult material followed the zone conventions in the adult skeleton. In other words, an unfused humerus would be missing the proximal and distal zones, and the unfused state would be recorded as PUF (proximal unfused) or DUF (distal unfused), or both, depending on the state of fusion, to separate it from a fragmented adult element preserving the same zones. Equally, unfused epiphyses were recorded by zones and as unfused.

Each fragment is recorded by all zones present, even if the zone is only a part of the whole, as well as from which bone, left or right, the fragment derives. The recorded fragments can then be used to aid conjoining exercises in cases where there is overlap in the zones of fragments. To aid use of this system, any of a number of standard anatomy texts can be used in conjunction with the diagrams of zones, such as the most recent edition of McMinn and Hutchings (1985).

Unidentifiable Fragments

In order to account for fragments too incomplete to be assigned to an individual element, we recommend employing Outram's (1998; 1999; 2001) method for recording these fragments. This system is based on a rough division of fragments into axial (e.g. largely cancellous bone tissue) or appendicular fragments (e.g. those with cancellous and cortical bone articulations) and then places them in size classes, after which individual counts are made based on those deriving from each unit or context. All fragments, including those fragments that cannot be assigned to either element or taxon, are assigned to a fragment size category. The size categories are based upon the maximum dimension and are as

follows: 0 – 20mm, 21 – 30mm, 31 – 40mm, 41 – 50mm, 51 – 60mm, 61 – 70mm, 71 – 80mm, 81 – 90mm, 91 – 100mm and 100+ mm. In order to facilitate rapid recording, circles can be drawn on paper with a compass such that individual fragments can be placed within them to determine the category in which they belong. Counting can be done manually, or for large groups, with finger-operated mechanical counters.

The nature of fracture type can also be recorded for each diaphysis fragment (Outram 1998; 1999; 2001; 2002). Bone breaks in predictably different ways depending upon whether the fracture occurred when the bone was still fresh, after a certain amount of drying but when the organic content is still present in some quantity, or when most organic content has been lost. Three principal criteria can be used to judge fracture type. These are fracture outline (shape of the fracture pattern), fracture angle to the cortical surface and fracture texture. These criteria can be employed either to produce a numerical index of fracture type within a continuum from totally fresh bone full of collagen to bones containing some collagen that produce 'dry fractures' through to totally mineralised bone with little or no collagen remaining (Outram 1998; 2002; see also Villa and Mahieu 1991; White 1992; Lyman 1994; Valentin and Le Goff 1998; Galloway 1999), or used more subjectively to identify presence or absence of given fracture types. This methodology is aimed at providing a general picture of the fracture history of the assemblage, based on large sample sizes, rather than on correctly identifying what happened to every individual bone in detail. The recording of fragmentation and fracture patterns in this way provides one with a powerful tool for the study of the taphonomy of complex mixed assemblages of human and animal remains. It allows one to compare and contrast the fracture and fragmentation histories of different archaeological contexts and compare the treatment of human and animal remains within those contexts.

The Zonation Method Applied to Humans

Zones were developed for the following elements: mandible (Fig. 1); vertebrae: cervical, thoracic, lumbar, and sacral vertebrae (Fig. 2); ribs (Fig. 3); scapula (Fig. 4); humerus (Fig. 5); radius (Fig. 6); ulna (Fig. 7); *Os coxae* (Fig. 8); femur (Fig. 9); tibia (Fig. 10); metapodials and phalanges (Figs. 11 and 12); calcaneus (Fig. 12); and talus (Fig. 12). New zones for elements not included in Dobney and Rielly's (1988) original article were as follows: cranium (Figs. 13, 14, 15, 16, 17 and 18); sternum (Fig. 19); clavicle (Fig. 20); and fibula (Fig. 21).

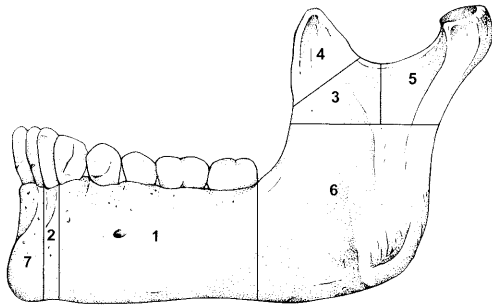
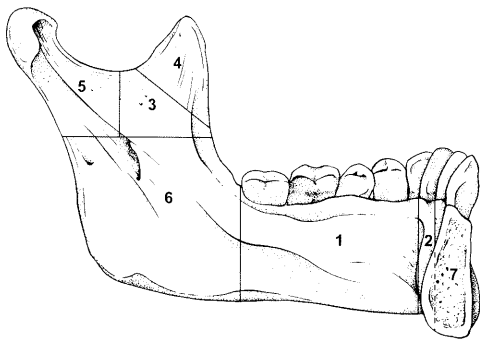
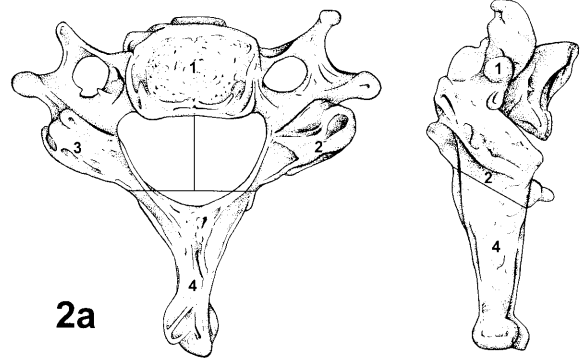
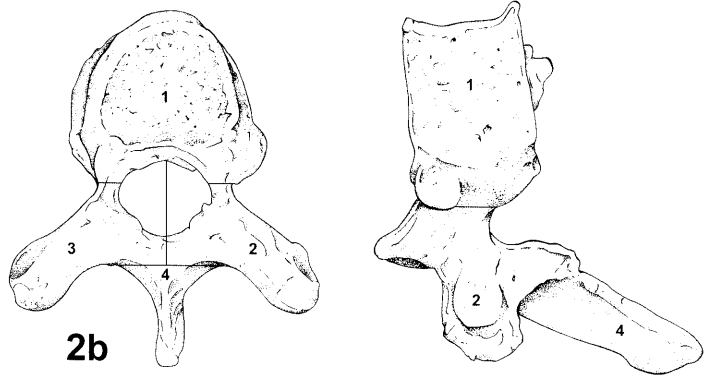


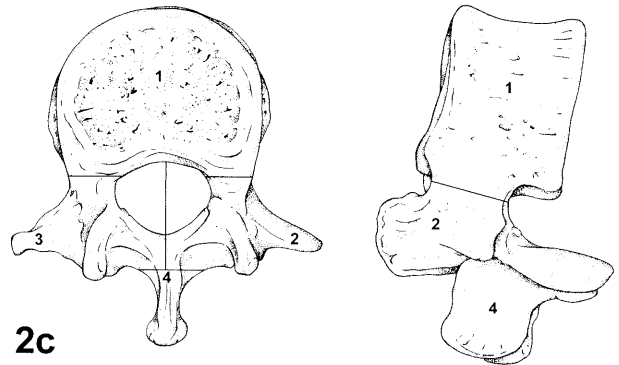
Figure 1. Mandible, medial (internal) and lateral (external) views: 1- the portion of the corpus, including the alveoli for the premolars and molars as well as the premolars and molars themselves; 2- the portion of the corpus, including the alveolus for the canine and the canine itself; 3- the area of the ascending ramus inferior to the coronoid process; 4- the coronoid process; 5- the posterior portion of the ascending ramus and the mandibular condyle; 6- the gonial angle, including the mandibular foramen and mylohyoid groove (internally) and the attachment of M. masseter (externally); 7- the anterior portion of the corpus, including the alveoli of the incisors and the incisors themselves.



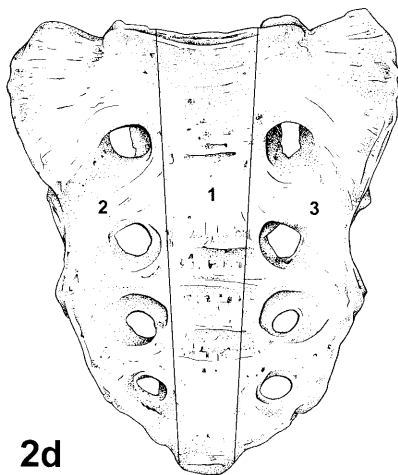
2a



2b



2c



2d

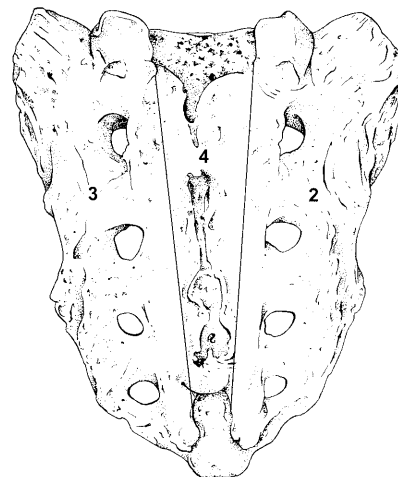


Figure 2. Vertebrae: (a) Cervical vertebrae, superior and right lateral views; (b) Thoracic vertebrae, superior and right lateral views; (c) Lumbar vertebrae, superior and right lateral views; (d) Sacral vertebrae, ventral and dorsal views. 1- the body; 2- the right transverse process, including the pedicle, pars interarticularis, and articular facets; 3- the left transverse process, including the pedicle, pars interarticularis, and articular facets; 4- the spinous process.

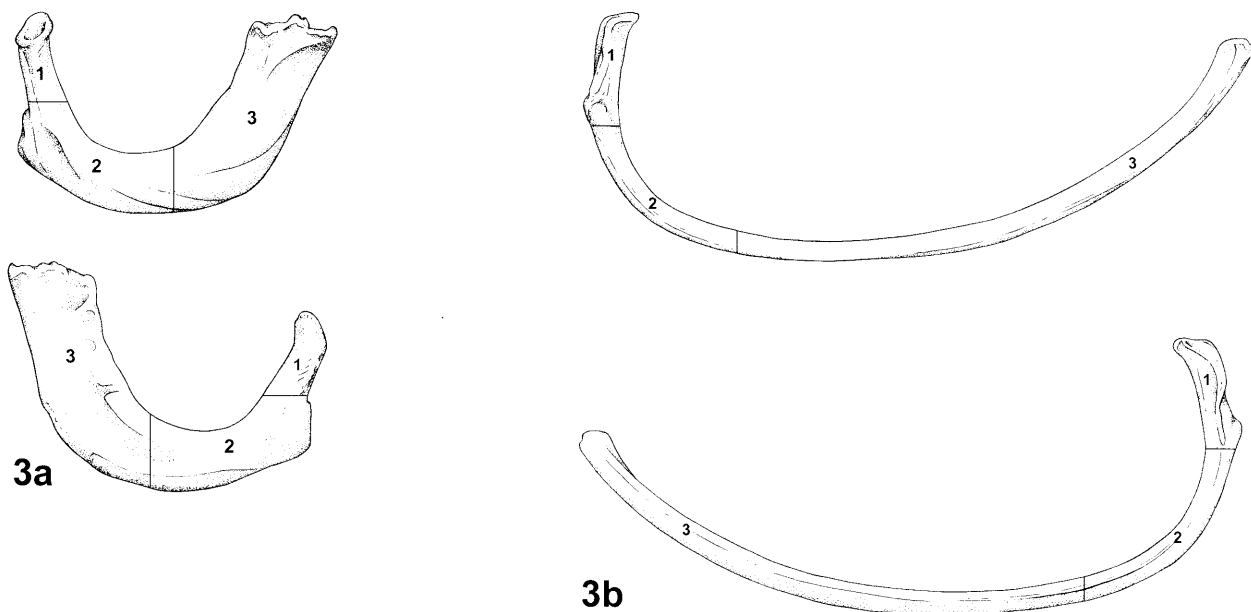


Figure 3. Ribs, inferior and superior views: (a) Rib 1; (b) Rib 7. 1– the head; 2– the area of the angle of the rib, including the articular and non-articular costal facets in ribs 1 through 10; 3– the remaining corpus and sternal end.

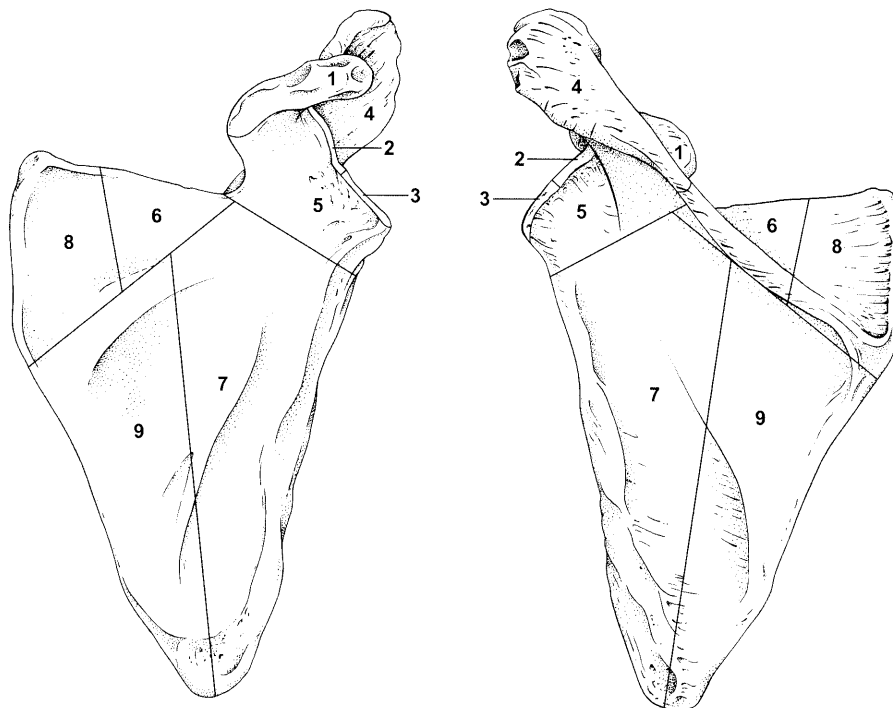


Figure 4. Scapula, ventral and dorsal views: 1– the coracoid process; 2– the superior half of the glenoid cavity; 3– inferior half of the glenoid cavity; 4– the acromial end and the axillary third of the spine; 5– the axillary third of the squamous portion and spine, including the neck and the area inferior to the coracoid process; 6– the middle third of the squamous portion superior to the spine and the middle portion of the spine, as well as the adjoining portion of the supraspinous fossa; 7– the axillary half of the squamous portion inferior to the spine, including the infraspinous fossa; 8– the vertebral third of the squamous portion and spine, including the attachment for *M. rhomboideus major* and supraspinous fossa; 9– the vertebral half of the squamous portion inferior to the spine, including the infraspinous fossa.

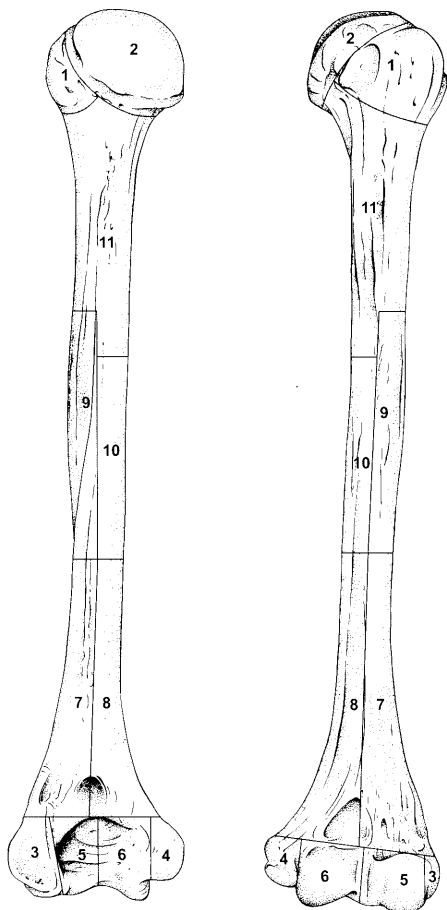


Figure 5 (left): Humerus, posterior and anterior views: 1– the greater and lesser tubercles; 2– the caput; 3– the lateral epicondyle; 4– the medial epicondyle; 5– the lateral articular process (capitulum) of the condyle; 6– the medial articular process (trochlea) of the condyle; 7– the distal lateral half of the diaphysis, including one-half of the olecranon fossa and the radial fossa; 8– the distal medial half of the diaphysis, including one-half of the olecranon fossa and the coronoid fossa, including the nutrient foramen; 9– the area surrounding the deltoid tuberosity; 10– the area opposite 9 making up one-half of the diaphysis longitudinally in the sagittal plane and cutting the bone transversely from medial to lateral; 11– the proximal portion of the diaphysis, including the surgical neck.

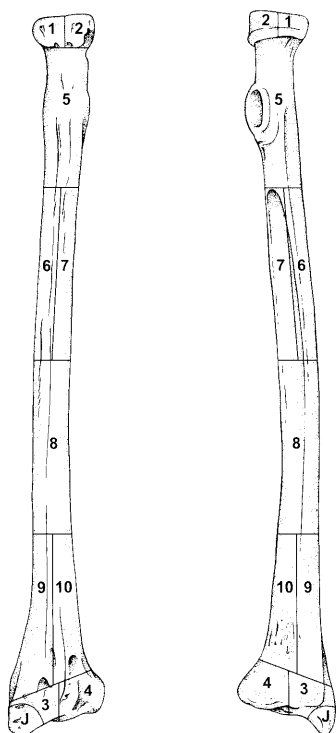


Figure 6 (left). Radius, posterior and anterior views: 1– the lateral half of the radial head; 2– the medial half of the radial head; 3– the lateral portion of the distal articulation; 4– the medial portion of the distal articulation; 5– the proximal portion of the diaphysis, including the radial tuberosity; 6– the lateral half of the diaphysis to the mid-point of the diaphysis, including the attachment for *M. pronator teres*; 7– the medial half of diaphysis to the mid-point of the diaphysis, opposite zone 6, including the nutrient foramen, which is located antero-medially; 8– the superior half the distal third of the radius; 9– the lateral distal third of the diaphysis; 10– the medial distal third of the diaphysis; J– the styloid process of the distal end.

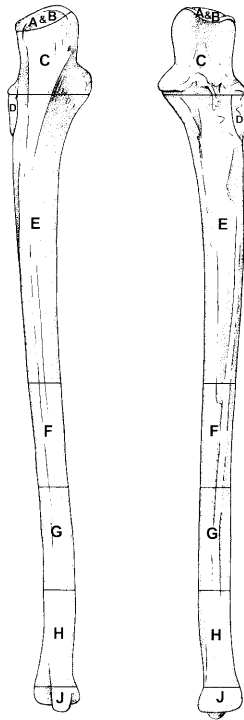


Figure 7 (left). Ulna, posterior and anterior views: A and B— the olecranon process; C— the area of the trochlear or semi-lunar notch, including the coronoid process; D— the radial notch; E— the proximal half of the diaphysis distal to area C, including the nutrient foramen, which is located antero-medially; F— the middle portion of the shaft; G— the superior one-half of the distal third of the diaphysis; H— the distal half of the distal third of the shaft, including the attachment of M. pronator quadratus; J— the styloid process and head, including the posterior groove for M. extensor carpi ulnaris.

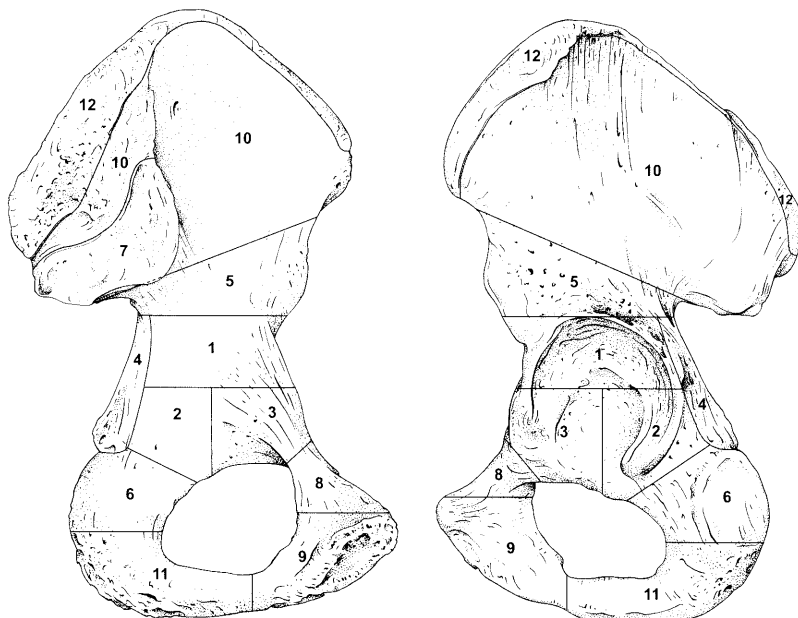


Figure 8 (left). Os coxae, medial (internal) and lateral (external) views: 1— the superior portion of the acetabulum and adjoining areas anteriorly and posteriorly; 2— the posterior half of the inferior portion of the acetabulum and adjoining areas; 3— the anterior half of the inferior portion of the acetabulum and adjoining areas; 4— the superior portion of the ischium, including the ischial spine; 5— the inferior portion of the ilium, including the greater sciatic notch; 6— superior portion of the ischial tuberosity; 7— the auricular surface of the ilium; 8— the superior portion of the pubis possessing the pectineal line and pubic tubercle; 9— the inferior portion of the pubis, including the pubic symphysis; 10— the greater part of the ilium, marked in an antero-posterior direction by a line running from just inferior to the anterior superior iliac spine to the posterior inferior iliac spine, but not including the iliac crest (superiorly); 11— the inferior portion of the ischium, including the majority of the ischial tuberosity; 12— the iliac crest.

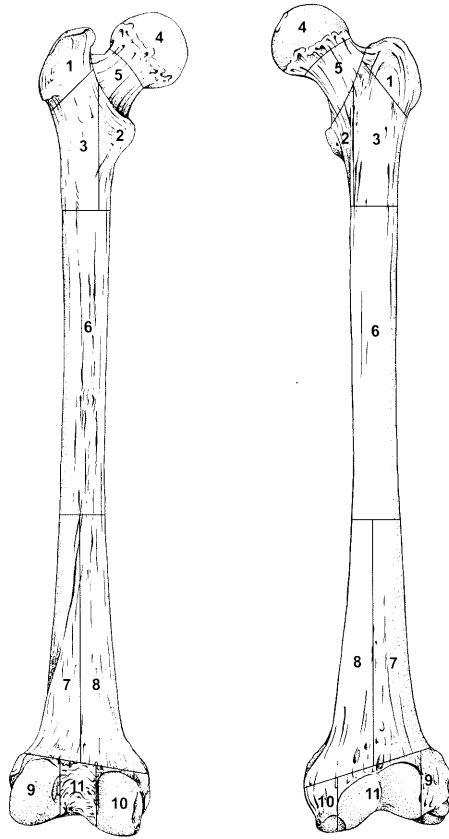


Figure 9 (left). Femur, posterior and anterior views: 1— the greater trochanter; 2— the area around the lesser trochanter and the lesser trochanter; 3— the area of the cranial attachment of *M. gluteus maximus*; 4— the caput; 5— the neck of the element and area along the intertrochanteric line (anteriorly) and intertrochanteric crest (posteriorly); 6— the middle portion of the diaphysis to the point where the linea aspera bifurcates into the supra-condylar lines, including the nutrient foramen, which is located posteriorly; 7— the lateral half of the distal third of the diaphysis split longitudinally in the sagittal plane, including one-half of the popliteal space (posteriorly); 8— the medial half of the distal third of the diaphysis split longitudinally in the sagittal plane, including one-half of the popliteal space (posteriorly); 9— the lateral condyle and epicondyle; 10— the medial condyle and epicondyle; 11— the intercondylar space and distal articulation anteriorly.

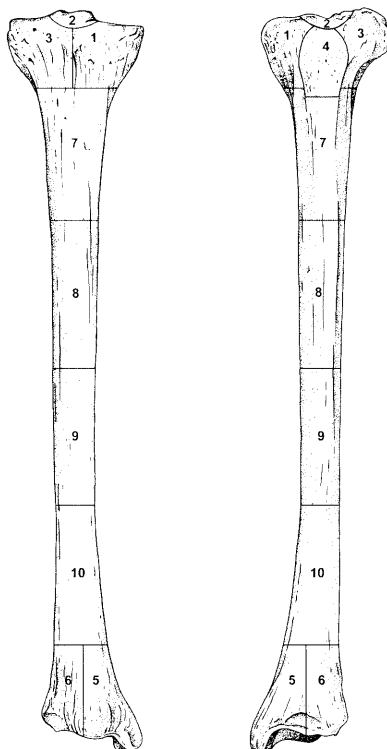


Figure 10 (left). Tibia, posterior and anterior views: 1— the medial proximal condyle; 2— the intercondylar fossa between the tibial spines, including the area of attachment of the posterior cruciate ligament; 3— the lateral proximal condyle; 4— the area of the tibial tuberosity; 5— the area of the medial malleolus; 6— the area of the lateral malleolus; 7— the proximal quarter of the diaphysis, including the nutrient foramen, posteriorly; 8— the second quarter of the diaphysis; 9— the third quarter of the diaphysis; 10— the distal quarter of the diaphysis.

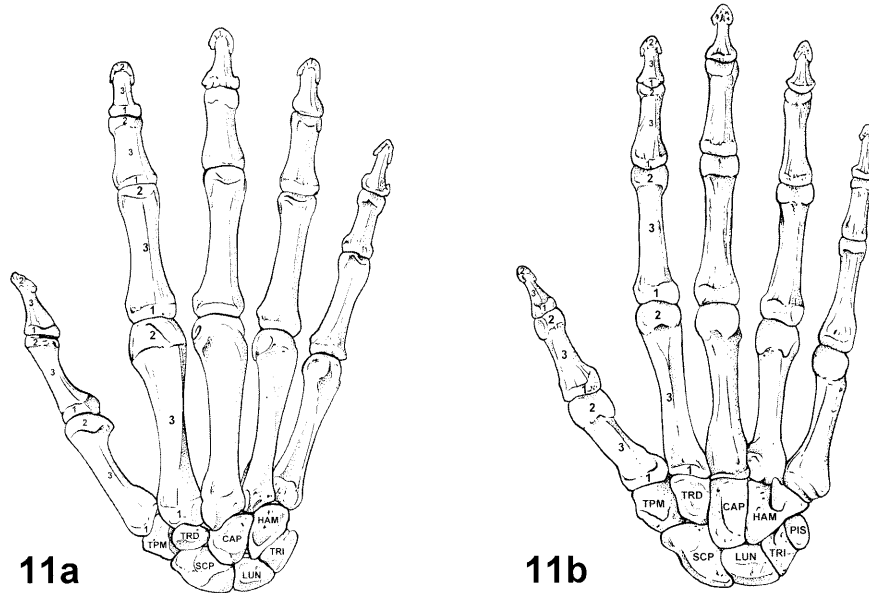


Figure 11. The hand and wrist: (a) dorsal view; (b) palmar view. Metapodials and phalanges: 1– the proximal articulation; 2– the distal articular condyle; 3– the diaphysis. Carpals: TPM– trapezium; TRD– trapezoid; CAP– capitae; HAM– hamate; SCP– scaphoid; LUN– lunate; TRI– triquetral.

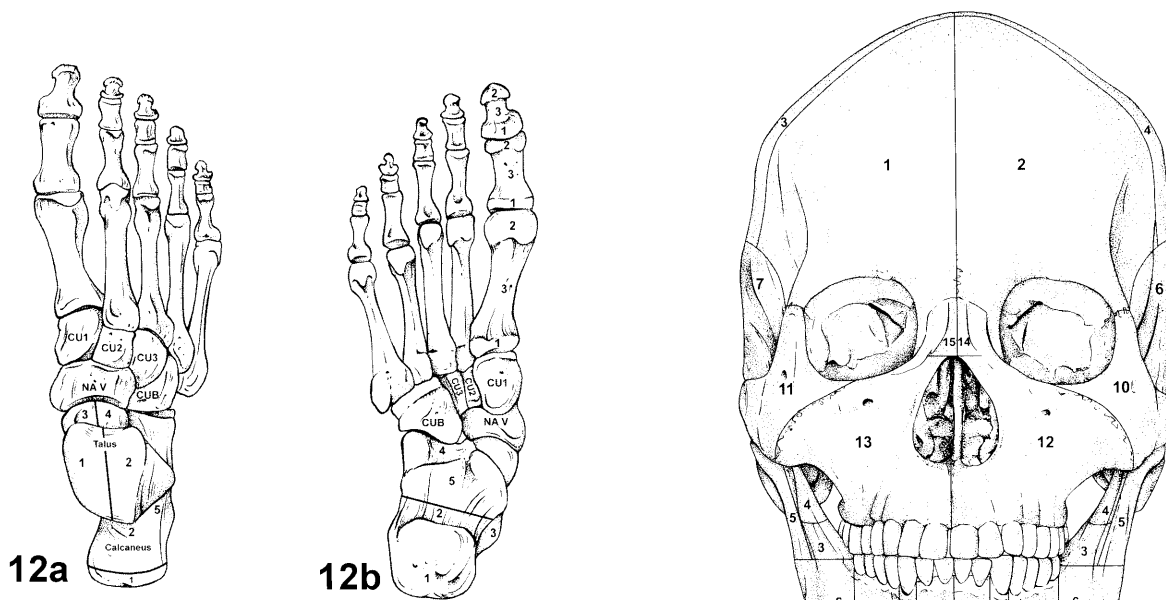


Figure 12. The foot and ankle: (a) dorsal view; (b) plantar view. Calcaneus: 1– the tuber calcis; 2–the distal portion of the body; 3– the sustentaculum tali; 4– the proximal articulation; 5– the proximal portion of the body inferior to the articulations. Talus: 1– medial half of the trochlea; 2– lateral half of the trochlea; 3– medial half of the proximal portion, splitting the head sagittally; 4– lateral half of the proximal portion, splitting the head sagittally. Metapodials and phalanges: 1– the proximal articulation; 2– the distal articular condyle; 3– the diaphysis. Tarsals: CU1– medial cuneiform; CU2– intermediate cuneiform; CU3– lateral cuneiform; NAV– navicular; CUB – cuboid.

Figure 13: Cranium, Norma facialis: 1– the right frontal, split sagittally through the metopic suture; 2– the left frontal, split sagittally through the juvenile metopic suture; 3– the right parietal; 4– the left parietal; 6– the left temporal, including the root of the zygomatic process from the left side; 7–the right temporal, including the root of the zygomatic process from the right side; 10– the left zygoma; 11– the right zygoma; 12– the left maxilla; 13– the right maxilla; 14– the left nasal bone; 15– the right nasal bone.

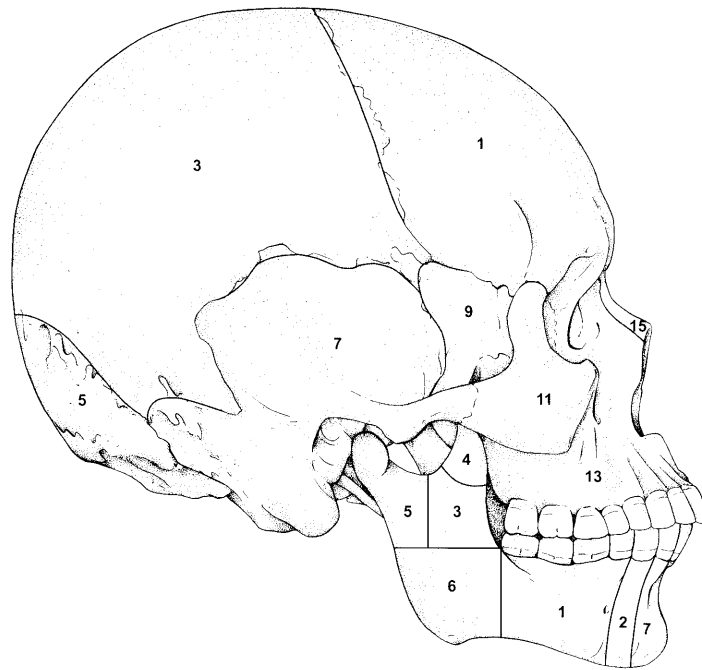


Figure 14. Cranium, *Norma lateralis dextra*: 1– the right frontal, split sagittally through the metopic suture; 3– the right parietal; 5– the occipital; 7– the right temporal, including the root of the zygomatic process from the right side; 9– the right sphenoid; 11– the right zygoma; 13– the right maxilla; 15– the right nasal bone.

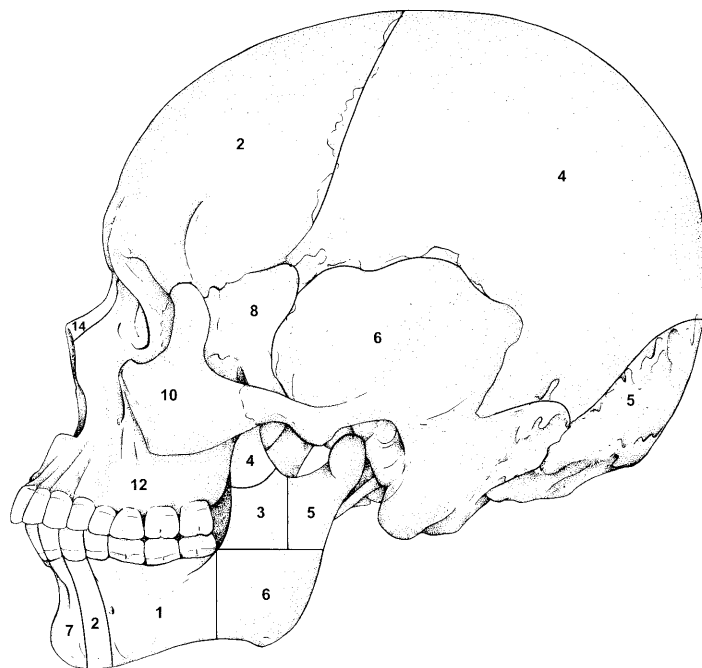


Figure 15. Cranium, *Norma lateralis sinistra*: 2– the left frontal, split sagittally through the metopic suture; 4– the left parietal; 5– the occipital; 6– the left temporal, including the root of the zygomatic process from the left side; 8– the left sphenoid; 10– the left zygoma; 12– the left maxilla; 14– the left nasal bone.

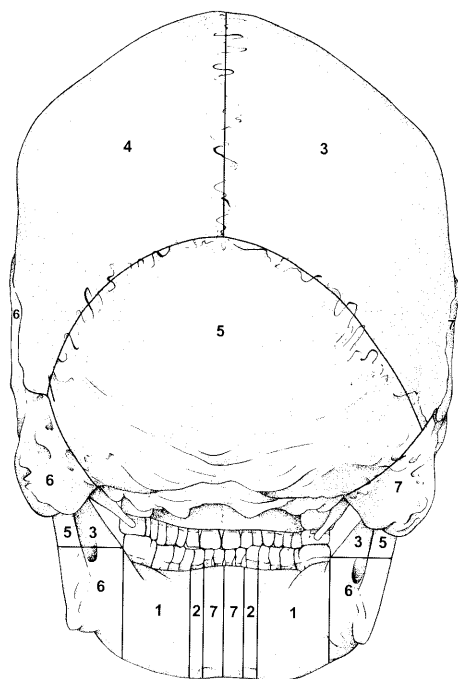


Figure 16. Cranium, Norma occipitalis: 3- the right parietal; 4- the left parietal; 5- the occipital; 6- the left temporal, including the root of the zygomatic process from the left side; 7- the right temporal, including the root

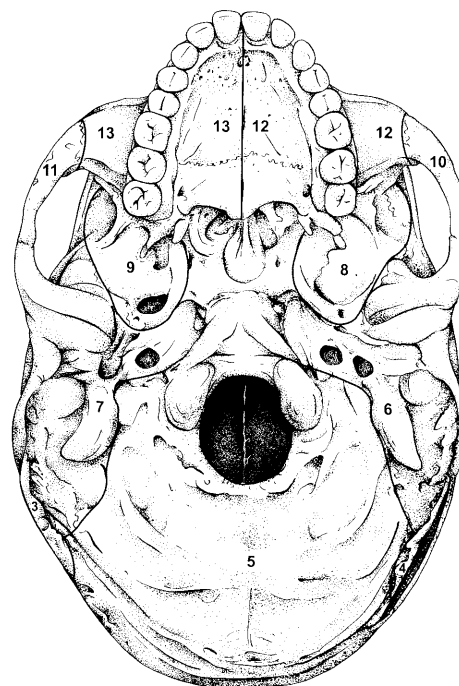


Figure 18. Cranium, Norma basalis: 3- the right parietal; 4- the left parietal; 5- the occipital; 6- the left temporal, including the root of the zygomatic process from the left side; 7- the right temporal, including the root of the zygomatic process from the right side; 8- the left sphenoid; 9- the right sphenoid; 10- the left zygoma; 11- the right zygoma; 12- the palatal process of the left maxilla; 13- the palatal process of the right maxilla.

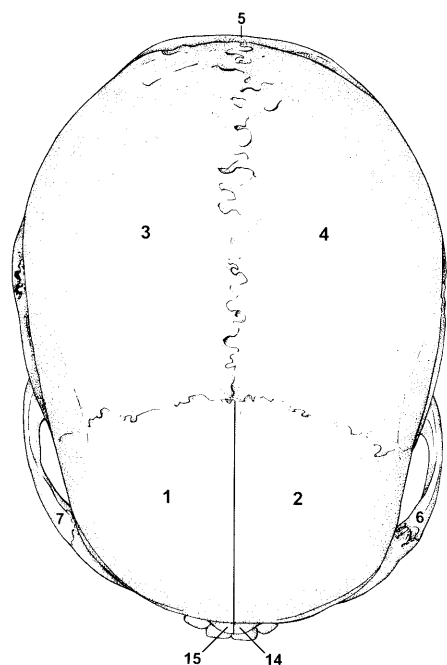


Figure 17. Cranium, Norma verticalis: 1- the right frontal, split sagittally through the metopic suture; 2- the left frontal, split sagittally through the metopic suture; 3- the right parietal; 4- the left parietal; 5- the occipital; 6- the left temporal, including the root of the zygomatic process from the left side; 7- the right temporal, including the root of the zygomatic process from the right side; 14- the left nasal bone; 15- the right nasal bone.

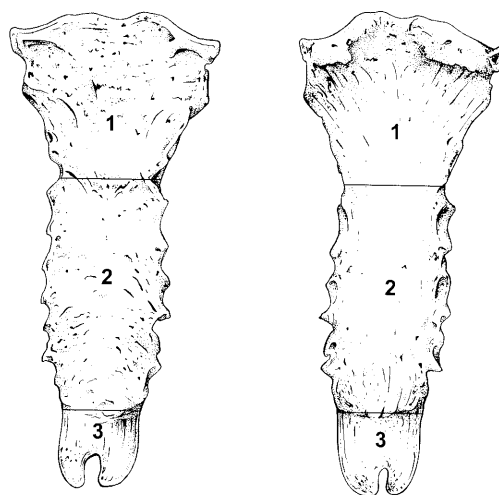


Figure 19. Sternum, anterior and posterior views: 1- the manubrium; 2- the corpus sterni; 3- the xiphoid process.

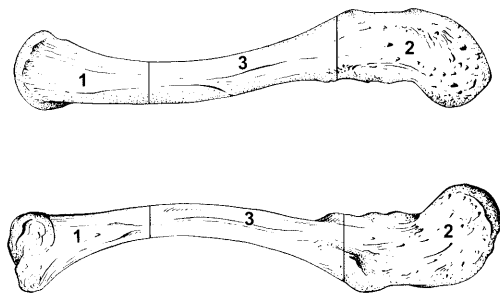


Figure 20. Clavicle, superior and inferior views: 1– the sternal end, including the area of the attachment for the costo-clavicular ligament; 2– the acromial end, including the conoid tubercle and trapezoid line, the attachments for the two components of the coraco-clavicular ligament; 3– the diaphysis, including the groove which marks the attachment for *M. subclavius*.

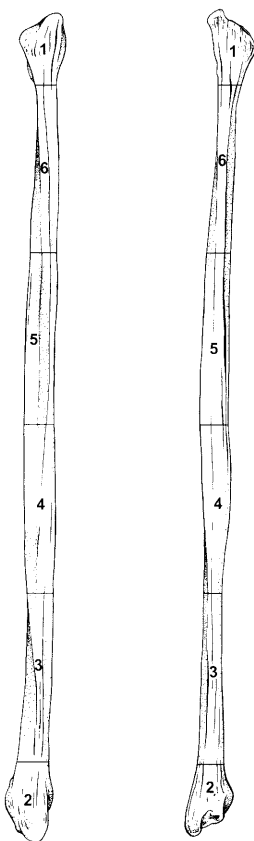


Figure 21. Fibula, anterior and posterior views: 1– the proximal end, essentially the juvenile epiphysis, including the styloid process; 2– the distal end, essentially the juvenile epiphysis; 3– the most distal quarter of the diaphysis, including the attachment for the inferior portion of the interosseous ligament (a triangular rugose region with its apex directed anteriorly); 4– the middle quarter of the diaphysis, including the nutrient foramen, which is located posteriorly; 5– the second quarter of the diaphysis; 6– the most proximal quarter of the diaphysis, distal to the juvenile epiphysis.

Conclusion

We anticipate that this recording system, or modified versions of it, will lead to more robustly defensible inferences drawn from assemblages of human remains and, specifically, to address questions exploring the similarity of human and non-human treatment from the past in the present.

Acknowledgements

The authors thank the Velim Skalka, Czech Republic, research team for their contributions to the project from whence this contribution sprang: Prof. Anthony F. Harding (Durham), Dr. Stephanie Knight (Wessex Archaeology), Rebecca Craig (Bradford), and Dr. Carol Palmer (Sheffield). We thank the Archaeological Institute of the Czech Academy of Sciences and, specifically, Radka Sumberová for providing space and logistical support for the work. Anthony Harding directed the excavation of the English Expedition's portion of the Velim Skalka site, and the team completed the analysis of human and animal bones from this excavation under the auspices of Leverhulme Trust Grant F/00 235/B. Caroline D. Needham, of the Unit of Medical Art in Medicine, University of Manchester, drew the figures of the zones, and her time and expertise was made available through British Academy Grant SG-36744.

Notes

- 1 Louise Loe from Bournemouth University, who has employed the human zonation system recently, has further divided the cranial zones by adding separate zones for the basilar process of the occipital and one each for the two petrous temporal bones. She has also combined zones 4 and 5 of the fibula due to the inherent difficulties in distinguishing diaphyseal fragments in this element.

References

- Binford, L. R. 1984. *Faunal Remains from Klasies River Mouth*. New York: Academic Press.
- Buikstra, J. E. and Ubelaker, D. H. (eds.) 1994. *Standards for Data Collection from Human Skeletal Remains*. Fayetteville, Arkansas: Arkansas Archaeological Survey.
- Carr, G. C. and Knüsel, C. J. 1997. An assessment of the evidence for exposure burial in the Iron Age of southern England, pp. 167–73 in Gwilt, A. and Haselgrove, C. (eds.), *Reconstructing Iron Age Societies: New Approaches to the British Iron Age* (Oxbow Monograph 71). Oxford: Oxbow Books.
- Dobney, K. M. and Rielly, K. 1988. A method for recording archaeological animal bones: the use of diagnostic zones. *Circaea* 5, 79–96.
- Galloway, A. 1999. *Broken Bones: Anthropological Analysis of Blunt Force Trauma*. Springfield, Illinois: Charles Thomas.

- Klein, R. G. and Cruz-Urbe, K. 1984. *The Analysis of Animal Bones from Archaeological Sites*. Chicago: University of Chicago Press.
- Lyman, R. L. 1994. *Vertebrate Taphonomy* (Cambridge Manuals in Archaeology). Cambridge: Cambridge University Press.
- McMinn R. H. M. and Hutchings, R. T. 1985. *Color Atlas of Human Anatomy*. Chicago: Year Book Medical Publishers.
- Morlan, R. E. 1994. Bison bone fragmentation and survivorship: a comparative method. *Journal of Archaeological Science* **21**, 797–807.
- Outram, A. K. 1998. *The Identification and Palaeoeconomic Context of Prehistoric Bone Marrow and Grease Exploitation*. Unpublished PhD thesis, University of Durham.
- Outram, A. K. 1999. A comparison of paleo-Eskimo and Medieval Norse bone fat exploitation in Western Greenland. *Arctic Anthropology* **36**, 103–17.
- Outram, A. K. 2001. A new approach to identifying bone marrow and grease exploitation: why the 'indeterminate' fragments should not be ignored. *Journal of Archaeological Science* **28**, 401–10.
- Outram, A. K. 2002. Bone fracture and within-bone nutrients: an experimentally based method for investigating levels of marrow extraction, pp. 51–63 in Miracle, P. and Milner, N. (eds.), *Consuming Passions and Patterns of Consumption* (McDonald Institute Monograph Series). Cambridge: McDonald Institute.
- Valentin, F. and Le Goff, I. 1998. La sépulture mésolithique de La Chaussée Tirancourt: fracture sur os frais ou sur os secs? *L'Anthropologie* **1**, 91–5.
- Villa, P. and Mahieu, E. 1991. Breakage patterns of human long bones. *Journal of Human Evolution* **21**, 27–48.
- White, T. D. 1992. *Prehistoric Cannibalism at Mancos 5MTUMR-2346*. Princeton, New Jersey: Princeton University Press.